Clinical Characteristics and Kidney Outcomes in Chinese Patients with Autosomal Dominant Polycystic Kidney Disease

Winston Wing-Shing Fung[1,2] *Cheuk-Chun Szeto*[1,2,3] *Kai-Ming Chow*[1,2] *Phyllis Mei-Shan Cheng*[1,2] *Vickie Wai-Ki Kwong*[1,2] *Sam Lik-Fung Lau*[1,2] *Wing-Fai Pang*[1,2] *Winnie Chiu-Wing Chu*[4] *Albert Chee Meng Ong*[5] *Olivier Devuyst*[6,7] *and Philip Kam-Tao Li*[1,2]

Key Points

- The Mayo clinic imaging classification allows more accurate risk stratification but is limited by the lack of data on non-White populations and on atypical imaging patterns.
- In this cohort of Chinese patients with autosomal dominant polycystic kidney disease, an atypical imaging pattern was observed in 17% of the cases, associated with later presentation and a milder disease course.
- There may be genotypic differences, especially among those with atypical imaging. Future genotyping studies will help to define the genetic basis for the phenotypic spectrum in Chinese patients.

Abstract

Background The management of autosomal dominant polycystic kidney disease (ADPKD) remains challenging with variable and uncertain genotype–phenotype correlations. The Mayo clinic imaging classification allows more accurate risk stratification but is limited by the atypical imaging patterns. We aim to assess the clinical characteristics and the morphology of the cystic kidneys in a cohort of Chinese patients with ADPKD.

Methods Ninety-eight patients with ADPKD were recruited prospectively from August 2019 to December 2020 in Prince of Wales Hospital, Hong Kong. They were subsequently followed up every 6 months for a minimum of 2 years. We reviewed the clinical characteristics and magnetic resonance imaging patterns at baseline and the kidney outcome at the end of the follow-up. Atypical imaging patterns included unilateral, segmental, asymmetric, lopsided, and bilateral atrophy as defined by the Mayo Imaging Classification.

Results The mean age was 51.5±14.3 years, and the mean eGFR 68.7±27.5 ml/min per 1.73 m^2. The 98 patients included 36 male and 62 female. Seventy-six patients (77.6%) had a family history. Seventeen of the 98 (17.3%) patients had atypical imaging patterns. Compared with typical cases, atypical cases were older at the time of diagnosis (49.5±16.0 versus 33.0±13.0 years, $P < 0.001$) and at the time of starting antihypertensive medications (52.4±14.8 versus 39.7±11.0 years, $P = 0.001$) and were less likely to have a positive family history (58.8% versus 81.5%, $P = 0.042$). Patients with atypical patterns showed a lower eGFR decline compared with those with the typical pattern (−0.86±4.34 versus −3.44±4.07 ml/min per 1.73 m^2 per year, $P = 0.022$).

Conclusions In this cohort of Chinese patients with ADPKD, an atypical imaging pattern was observed in 17% of the cases, associated with later presentation and a milder disease course. Future genotyping studies will help to define the genetic architecture and the basis for the phenotypic spectrum in Chinese patients with ADPKD.

Kidney360 5: 715–723, 2024. doi: https://doi.org/10.34067/KID.0000000000000433

[1]Department of Medicine and Therapeutics, Prince of Wales Hospital, Hong Kong, China
[2]CUHK Carol and Richard Yu Peritoneal Dialysis Research Centre, Hong Kong, China
[3]Li Ka Shing Institute of Health Sciences (LiHS), The Chinese University of Hong Kong, Hong Kong, China
[4]Department of Imaging and Interventional Radiology, The Chinese University of Hong Kong, Hong Kong, China
[5]Academic Nephrology Unit, The University of Sheffield Medical School, Sheffield, United Kingdom
[6]Institute of Physiology, University of Zurich, Zürich, Switzerland
[7]Division of Nephrology, UCLouvain Medical School, Brussels, Belgium

Correspondence: Dr. Winston Wing-Shing Fung or Prof. Philip Kam-Tao Li, email: fws898@ha.org.hk or philipli@cuhk.edu.hk

Received: September 26, 2023 **Accepted:** March 26, 2024
Published Online Ahead of Print: April 1, 2024

Introduction

Autosomal dominant polycystic kidney disease (ADPKD) is the most common hereditary kidney disease, accounting for about 10% of prevalent patients with kidney failure.[1] It is characterized by the development of multiple progressively enlarging kidney cysts which eventually replace healthy tissue, leading to kidney failure.[2] The diagnosis of ADPKD is primarily based on family history, clinical examination, and ultrasound imaging criteria, which can be complemented by magnetic resonance imaging (MRI) and genetic analysis.[3] Determining individual prognosis in ADPKD remains a challenge as the presentation and rate of progression can vary significantly between and within affected families.[4] This heterogeneity may lead to a delay in providing effective management to slow disease progression and to prevent associated complications. Therefore, there is an unmet need to establish accurate risk stratification at early stages of the disease, such that disease-modifying treatment, such as tolvaptan, can be instigated promptly, especially for those at-risk for rapid progression, to enable the most effective intervention before severe disease progression.[5]

One such risk prediction tool is the Mayo clinic imaging classification[6] based on the height-adjusted total kidney volume (Ht-TKV) obtained by MRI—an independent predictor of the risk of kidney disease progression in patients with ADPKD.[7,8]

However, the Mayo clinic imaging classification has some limitations. First, it deals with two distinctive morphological patterns of ADPKD on MRI.[6] There are those with typical morphology (class 1), as defined by diffuse bilateral cystic involvement and enlargement of the kidneys, and those with atypical morphology (class 2), as defined by one the following imaging patterns: (*1*) unilateral, (*2*) asymmetric, (*3*) segmental, (*4*) lopsided, or bilateral cystic disease with (*5*) unilateral or (*6*) bilateral kidney atrophy.[6] These two imaging patterns may correspond to different genotypes and clinical characteristics. Indeed, although the Mayo clinic imagining classification is validated for predicting the risk of rapid progression, it currently applies only to class 1 patients with typical morphology,[6] and there are currently no validated prediction tools for class 2 patients. Second, the data used for the development of the Mayo clinic imaging classification have been largely obtained from White populations,[6,9] although this imaging classification has been subsequently been validated in non-White populations.[10] The clinical course, the genotype–phenotype correlation, and the degree of heterogeneity in Asian ethnicities remains unclear. Particularly, patients with atypical kidney imaging patterns have not been well characterized in non-White populations.[10]

In this study, we aim to define the imaging characteristics and the clinical features of ADPKD in a Chinese cohort at baseline and whether the imaging patterns are associated with specific presentations and outcomes. The possibility to identify predictors of rapid disease progression at early stages of ADPKD is crucial for the selection of patients who will benefit the most from new therapies.[11]

Methods

This was a prospective observational study conducted at a single center. Unrelated, adult patients with clinical diagnosis of ADPKD based on imaging[3] and family history were recruited from our renal clinic between August 2019 and December 2020. Patients with an eGFR <30 ml/min per 1.73 m^2 (CKD Epidemiology Collaboration formula) or already on RRT were excluded. At the initial clinic visit after recruitment, baseline clinical data and biochemical parameters were collected. Baseline physical examination would include weight, height, BP, and abdominal girth. Detailed family history involving first-degree and second-degree relatives have also been recorded. A family history is defined as positive if any of these relatives are also affected by ADPKD.

Patients were followed-up routinely every 6 months as per our protocol or earlier if clinically indicated (such as rapidly worsening in kidney function) for a minimum of 2 years. The clinical data and biochemical parameters were collected at each follow-up visit. These include blood tests and eGFR measurement. Common symptomatology, such as abdominal pain, distension, and urinary symptoms, is also recorded systemically in each visit. An MRI was also

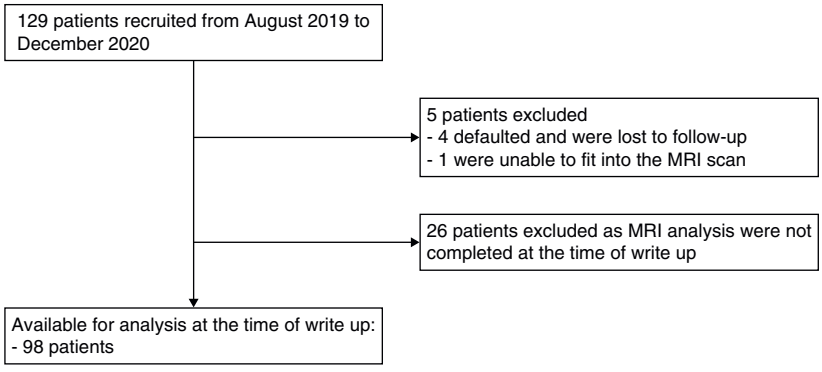

Figure 1. Flow diagram of the study population. One hundred and twenty-nine patients were recruited between August 2019 and December 2020, with 98 patients available for analysis. Five patients were excluded, and 26 patients did not have their MRI analysis completed. MRI, magnetic resonance imaging.

Table 1. Demographic and baseline clinical data

Parameters	No. of Patients (%)
Total	98
Sex male: female	36: 62
Age, yr[a]	51.5±14.3
Duration of follow-up, mo[a]	26.9±4.13
Age at diagnosis, yr[a]	35.8±14.8
Smoker, *No.* (%)	14 (14.3)
Comorbidities, *No.* (%)	
Diabetes	8 (8.2)
Hypertension	38 (38.8)
Hyperlipidemia	54 (55.1)
Ischemic heart disease	1 (1.0)
Stroke	3 (3.1)
Peripheral vascular disease	0 (0)
Respiratory disease	9 (9.2)
Cancer	8 (8.2)
Renal-related symptom/ manifestation, *No.* (%)	
Abdominal pain	36 (36.7)
Abdominal distension	25 (25.5)
Dysuria	2 (2.0)
Polyuria	13 (13.3)
Hematuria	11 (11.2)
Kidney stone	17 (17.3)
Urinary tract infection	9 (9.2)
Clinical parameters/ arthrometries	
Height, m[a]	1.64±0.09
Weight, kg[a]	62.9±11.4
Abdominal girth, cm[a]	87.4±10.8
BP, mm Hg[a]	132.9±16.9/82.6±11.4
MRI parameters	
Typical: Atypical, *No.* (%)	81 (82.7): 17 (17.3)
TKV, ml[b]	1072 (694–1617)
Ht-TKV, ml/m[b]	642 (432–1006)
Mayo class (1A: 1B: 1C: 1D: 1E)	11: 21: 28: 12: 9

Ht-TKV, height-adjusted total kidney volume; MRI, magnetic resonance imaging; TKV, total kidney volume.
[a]Expressed as mean±SD.
[b]Expressed as median (Interquartile range).

Table 2. Baseline biochemical parameters

XX (Normal Values)	No. of Patients (%)
Total	98
Hemoglobin, g/dl	12.77±1.55
White blood cell, $\times 10^9$/L	6.74±5.14
Platelet, $\times 10^9$/L	247.32±73.80
Sodium, mmol/L	140.44±2.48
Potassium, mmol/L	4.16±0.36
Urea, mmol/L	9.20±15.29
Creatinine, μmol/L	108.40±55.28
Total protein, g/L	74.94±4.36
Albumin, g/L	40.92±31.59
Bilirubin, μmol/L	8.85±4.00
Alkaline phosphatase, IU/L	71.79±23.12
Alanine aminotransferase, IU/L	24.59±11.78
Calcium, mmol/L	2.35±0.10
Phosphate, mmol/L	1.10±0.16
Urate, mmol/L	0.36±0.98
Osmolality, mOsm/kg	296.15±6.27
Urinary osmolality, mOsm/kg	418.23±161.28
Urinary protein:creatinine ratio, mg/mg Cr	0.66±4.78

All data are expressed as mean±SD.

performed after the first visit. The protocol of the MRI acquisition has been adapted from that used by the Euro-CYST consortium.[12] The acquisition protocol includes T2 single-shot fast/turbo spin-echo images with fat saturation, fast imaging with steady-state precession, or fast imaging employing steady-state acquisition 3D spoiled gradient echo and T1-3D spoiled gradient echo. The processing and the assessment of the MRI images were then performed by dedicated trained personnel using the program IntelliSpace Portal 9.0 workstation (Philips, Amsterdam, The Netherlands). The baseline Ht-TKV were calculated using the Mayo ellipsoid equation (total kidney volume [TKV] [ml]=$\pi/6\times$[length$\times$width$\times$depth]) or planimetry and the result be categorized according to the Mayo classification.[6] The length of the kidney is determined by averaging the maximum longitudinal diameters taken from the T2-weighted coronal and the sagittal plane while the depth and width of the kidney are determined on the T2-weighted axial plane. The various morphologies among the typical and atypical imaging patterns of ADPKD were also characterized according to the Mayo classification (Supplemental Table 1).[6] All participants were treated according to the standard of care in routine clinical practice. The age of starting antihypertensives was defined as the age at which any antihypertensives were started with a systolic BP of more than 140 mm Hg. The primary outcome was an assessment of kidney disease progression as defined by the slope of eGFR decline and a 40% decline from baseline eGFR.

Statistical analysis was performed by SPSS software version 27.0 (SPSS Inc., Chicago, IL). Descriptive statistics was used to describe the baseline characteristics of patients. Data are presented as mean±SD or median (interquartile range [IQR]) as appropriate. Difference between groups were compared by using the one-sample *t* test or Student *t* test as appropriate. Correlations between parameters were analyzed with Pearson rank correlation coefficients. Kaplan–Meier survival analysis was performed to assess the longitudinal association between the primary kidney event (*i.e.*, 40% decline from baseline eGFR, dialysis, or death) and the different Mayo subclasses. Differences between Kaplan–Meier curves were tested using the log-rank test. P values < 0.05 were considered statistically significant. All probabilities were two-tailed.

The study was approved by the Clinical Research Ethics Committee of the Chinese University of Hong Kong (Ref. No. 2018.421), and the study was performed in compliance with the Declaration of Helsinki.

Results

Ninety-eight patients with ADPKD recruited were available for analysis (Figure 1). Their baseline characteristics are summarized in Table 1. The mean age in the cohort is 51.5±14.3 years, and there was a female preponderance (1.72–1). The mean age at diagnosis is 35.8±14.8 years.

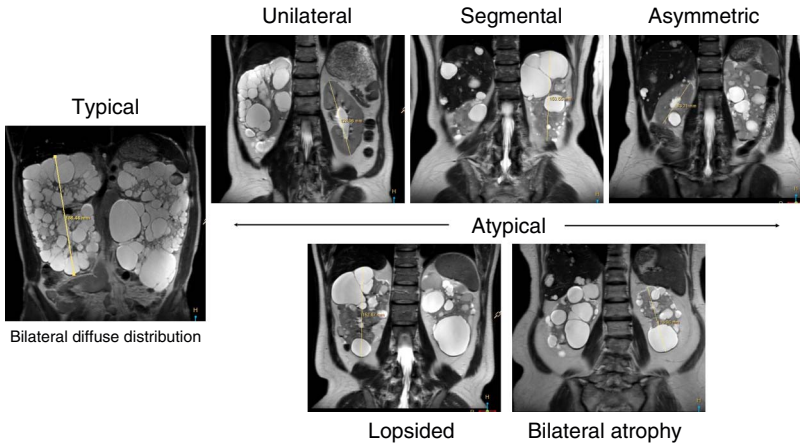

Figure 2. The illustrative examples of various atypical imaging morphologies in our Chinese cohort. Examples of images from our cohort showing various atypical imaging patterns according to the Mayo classification (Supplemental Table 1). Typical pattern with bilateral diffuse distribution of kidney cysts is shown on the left as a comparison.

Seventy-six patients (77.6%) had a positive family history. Seventy-four patients (75.5%) were on antihypertensive medications, including angiotensin-converting enzyme inhibitors/angiotensin II receptor blockers (59; 79.7%), β blockers (19; 25.7%), calcium channel blockers (36; 48.6%), and diuretics (7; 9.5%). No patients received tolvaptan. Most patients had abdominal pain and abdominal distension as the main symptoms, followed by hematuria and polyuria (Table 1).

The baseline biochemical parameters are shown in Table 2. The mean eGFR was 68.7±27.5 ml/min per 1.73 m^2, and the mean urinary osmolality was 418.23±161.28 mOsm/kg. The mean urine protein:creatinine ratio was 0.66±4.78 mg/mg Cr. Apart from reduced kidney function, no patients had anemia or liver derangement at baseline.

At baseline MRI, the median TKV was 1072 ml (IQR, 694–1617 ml), and the median Ht-TKV was 642 ml/m (IQR, 432–1006 ml/m). Of the 98 patients, 81 (82.7%) patients have a typical imaging pattern, and 17 (17.3%) patients have atypical pattern: unilateral (three cases), segmental (two cases), asymmetric (two cases), lopsided (nine cases), bilateral presentation with acquired unilateral atrophy (0 case), and bilateral presentation with bilateral kidney atrophy (one case). The various examples of the atypical pattern in our cohort are shown in Figure 2. As expected, mean Ht-TKV values were significantly different between the two patterns (1006.4±1064.5 versus 492.0±222.0 ml/m, $P < 0.001$). We performed a Pearson correlation analysis for urinary osmolality and Ht-TKV, but there was no significant correlation between urine osmolality and TKV. Conversely, there is a significant negative correlation between

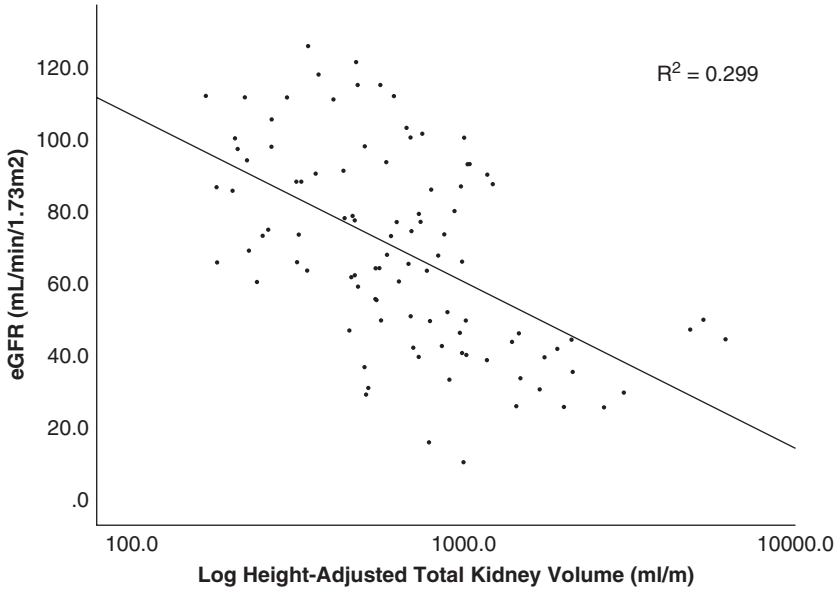

Figure 3. Scatterplot showing the correlation between $\log_{10}$ Ht-TKV and eGFR. There is a modest negative correlation between $\log_{10}$ Ht-TKV and eGFR with a R^2 −0.299. Ht-TKV, height-adjusted total kidney volume.

Table 3. Differences between typical and atypical imaging morphology

Parameter\Morphology (*No.*)	Typical (81)	Atypical (17)	*P* Value
Clinical			
Age at diagnosis, yr[a]	33.0±13.0	49.5±16.0	<0.001
Height, m[a]	1.64±0.09	1.60±0.08	0.082
Weight, kg[a]	63.1±12.1	62.3±8.2	0.811
Abdominal girth, cm[a]	87.5±10.8	86.9±11.2	0.833
Age starting antihypertensives, yr[a]	39.7±11.0	52.4±14.8	0.001
Positive family history, *No.* (%)	66 (81.5)	10 (58.8)	0.042
Symptomatology, *No.* (%)			
Abdominal pain	28 (34.6)	8 (47.1)	0.409
Abdominal distension	22 (27.2)	3 (17.6)	0.548
Polyuria	6 (7.4)	7 (41.2)	0.001
Dysuria	1 (1.2	1 (5.9)	0.318
Hematuria	10 (12.3)	1 (5.9)	0.683
Blood[a]			
Hemoglobin, g/dl	12.6±1.5	13.4±1.5	0.072
White blood cell, $\times 10^9$/L	6.8±5.6	6.3±1.7	0.687
Platelet, $\times 10^9$/L	243.1±74.6	266.7±68.8	0.235
Sodium, mmol/L	140.6±2.1	139.7±3.8	0.182
Potassium, mmol/L	4.2±0.4	4.2±0.4	0.979
Urea, mmol/L	8.0±3.4	6.5±1.7	0.006
Creatinine, μmol/L	112.78±59.06	87.53±23.02	0.005
Bilirubin, μmol/L	8.7±4.1	9.7±3.4	0.333
Alkaline phosphatase, IU/L	72.1±23.7	70.5±20.6	0.798
Alanine aminotransferase, IU/L	24.0±12.1	27.2±10.1	0.311
Albumin, g/L	37.7±5.1	37.9±2.6	0.837
Calcium, mmol/L	2.35±0.1	2.37±0.1	0.358
Phosphate, mmol/L	1.11±0.16	1.06±0.15	0.236
Urate, mmol/L	0.37±0.1	0.30±0.1	0.013
Osmolality, mOsm/kg	296.3±5.9	295.6±7.9	0.688
Urinary osmolality, mOsm/kg	403.3±159.1	487.4±157.6	0.051
Primary outcome[a]			
Slope of eGFR decline, ml/min per 1.73 m^2 per year	−3.44±4.07	−0.86±4.34	0.022
TKV, ml	1649.5±1713.9	788.6±357.0	<0.001
Ht-TKV, ml/m	1006.4±1064.5	492.0±222.0	<0.001

Ht-TKV, height-adjusted total kidney volume; TKV, total kidney volume.
[a]Data are expressed as mean±SD.

eGFR and Ht-TKV ($r=-0.416$, $P < 0.001$), and this is also shown in a scatterplot (Figure 3).

The clinical characteristic and biochemical parameters of the two morphological patterns at MRI are summarized in Table 3, and a trend of eGFR decline over time for all the cases with the two patterns is shown in Figure 4, A and B. Patients with an atypical imaging pattern tended to be older at the time of diagnosis and older at the time of starting an antihypertensive, compared with patients showing a typical pattern. There were no differences in terms of general symptoms. Importantly, patients with typical MRI pattern showed a significantly faster eGFR decline than those with atypical patterns (−3.44±4.07 versus −0.86±4.34 ml/min per 1.73 m^2 per year, $P = 0.022$). We have performed a linear regression model to further assess whether the slope of eGFR differs between the typical and atypical imaging patterns. The atypical imaging pattern has a significantly better slope of eGFR decline compared with the typical pattern (coefficient B, 2.58; 95% confidence interval, 0.38 to 4.78, $P = 0.022$). A positive family history was also more frequently detected in the patients with a typical MRI pattern compared with those with atypical pattern (81.5% versus 58.8%, respectively, $P = 0.042$).

Kaplan–Meier plots were used to analyze the association between the time to reach 40% eGFR decline among different Mayo subclasses as defined by risk of disease progression (*i.e.*, low risk: class 1A–B, high risk: class 1C–E, and atypical: class 2). There was a slight separation among the curves between the different groups, but this was not statistically significant (log-rank $P = 0.751$) (Figure 5), which is probably due to the small number of cases in each subclasses and the relatively short follow-up duration. Linear regression model was also done to assess the slope of eGFR decline among different Mayo subclasses (Table 4). Among the typical imaging cases, those with class 1E tended to have the worse kidney outcome compared with those with class 1A similar than for the original cohort used for the Mayo classification.[6] Patients presenting atypical patterns appeared to have a good prognosis in kidney survival, similar to those with class 1A.

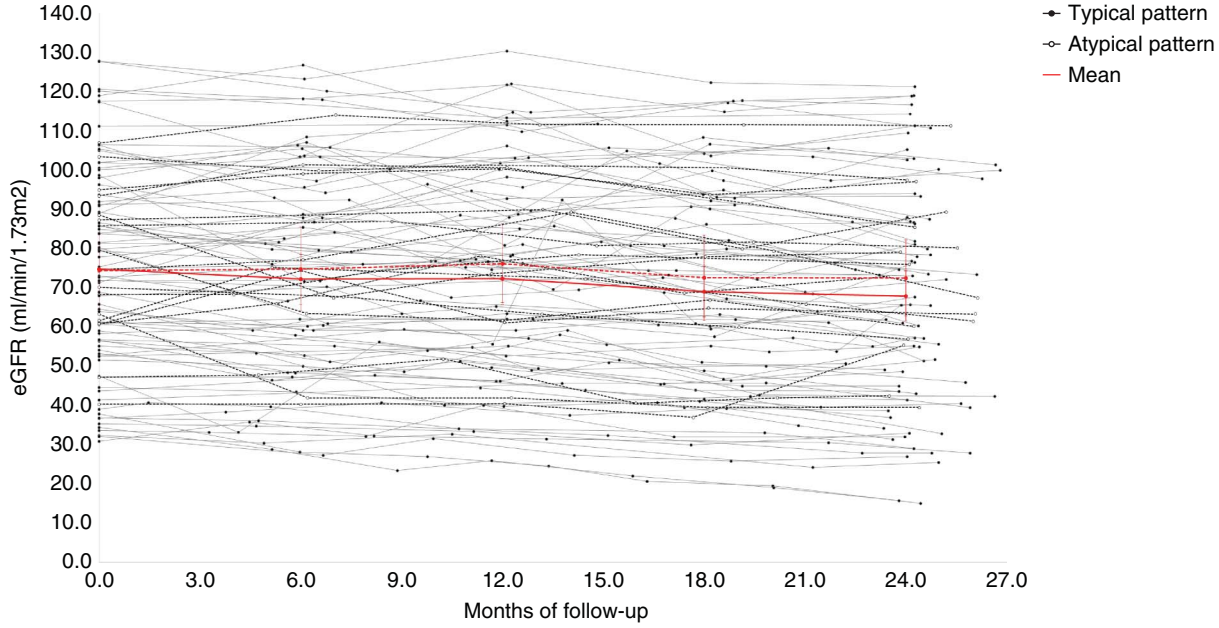

Figure 4. Trend of eGFR change over the entire observation period in individual patients with typical pattern and atypical pattern. Black circle with gray line denotes cases with typical pattern while white circle with dotted line denotes cases with the atypical pattern.

Discussion

Since the development of the Mayo clinic imaging classification, there is increasing interest in characterizing patients with ADPKD in Asia.[13] There is also increased focus on ADPKD research in China, and a specific clinical practice guideline for ADPKD in China has in fact been recently updated.[10,14] Similar to the study by Chen *et al.*,[10] our study aims to provide a detailed analysis of the clinical, biochemical, and imaging features of a large prospective cohort of patients with ADPKD in Asia. Comparing with the cohort from the Mayo Clinic Translational Polycystic Kidney Disease Center and the Consortium for Radiologic Imaging Studies of Polycystic Kidney Disease,[6] consisting of mostly White population, our cohort is older (median 51.7 versus 42 years, respectively) with a slightly lower eGFR (median 74.8 versus 78 ml/min per 1.73 m^2, respectively). Our cohort also had a higher Ht-TKV compared with the White cohort (642.2 versus 608 ml/m).

Although our current cohort is much smaller, it is interesting that our cohort appears to have a higher prevalence of atypical pattern compared with the previously reported Mayo cohort (17% versus 8.8%), which may be explainable by the difference in ethnicities or recruitment criteria between the two cohorts.[6,9] Furthermore, patients

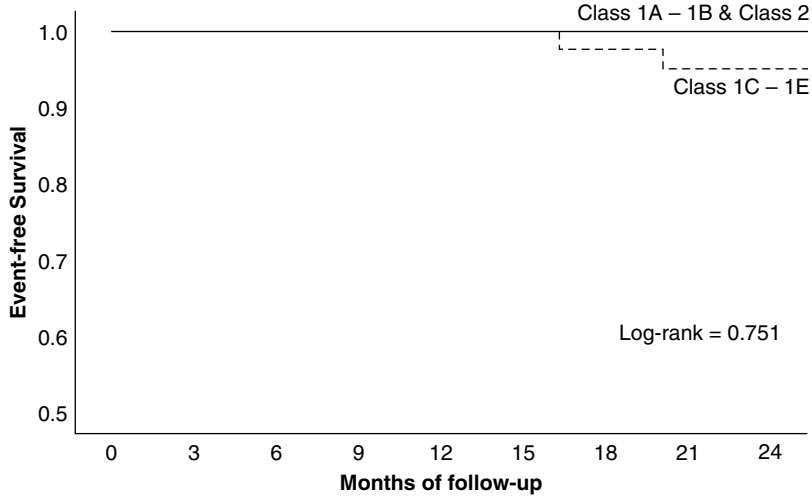

Figure 5. Kaplan–Meier curves showing 40% eGFR decline among various Mayo subclasses as defined by different risk of disease progression. Mayo class 1C–E seems to have a much higher risk of renal decline leading to a 40% drop of eGFR as compared with Mayo class 1A–B and the atypical image pattern (Mayo class 2). However, this was not statistically significant (log rank=0.751).

Table 4. Linear regression model on the slope of eGFR decline among different Mayo subclasses compared with the atypical pattern (class 2)

Mayo Subclasses	B Coefficient	95% Confidence Interval	*P* Value
Class 2	−0.864	−2.756 to 1.029	0.367
Class 1A	1.318	−1.702 to 4.338	0.388
Class 1B	−2.844	−5.419 to −0.269	0.031
Class 1C	−3.264	−5.718 to −0.811	0.010
Class 1D	−3.258	−6.278 to −0.238	0.035
Class 1E	−4.016	−7.234 to −0.799	0.015

with typical patterns seems to be more associated with a positive family history compared with those with atypical patterns in our cohort. However, detailed genotype analysis will be required to ascertain if these differences could relate to possible variations in genetic architecture in the Chinese ADPKD population or even novel genes. Indeed, a recent study in Taiwan showed that a specific PKD2 mutation (PKD2 p.Arg803* mutation) is the most common mutation in their ADPKD cohort, which suggested that a founder effect existed and has contributed to a major percentage of the ADPKD population in Taiwan.[15] This study certainly highlighted the importance of detailed genotyping in our cohort with a higher prevalence of atypical patterns, which may shed light on genetic difference among Chinese to White ADPKD population.

Our study showed that patients with the two imaging classes have different clinical characteristics. Those with atypical imaging patterns tended to be older at diagnosis and at the time of needing antihypertensive. The atypical patterns also have a seemingly better kidney outcome compared with those with a typical pattern. In essence, the two imaging patterns may represent two distinct phenotypic spectrums in our ADPKD cohort. The better characterization of atypical patterns from the typical patterns would be important because failure to recognize patients with atypical patterns may invalidate the Mayo classification and lead to erroneous risk stratification. In fact, efforts to develop a revised model that allows inclusion of atypical cases to develop a better prediction model are ongoing.[16,17]

Mutations in *PKD1* (coding for polycystin-1) and *PKD2* (coding for polycystin-2) account for approximately 80% and 15% of cases of ADPKD, respectively.[18] Recently, a number of rarer genes such as *GANAB* (encoding glucosidase II Alpha Subunit), *DNAJB11*, *ALG5*, *ALG9*, and *IFT140* have been identified: These result in a milder phenotype or a phenotype with predominant polycystic liver disease.[19–24] It is possible that some of the atypical imaging patterns may be caused by these genetic mutations.

It has been hypothesized that sporadic cases with the *de novo* mutations are one of the causes for the atypical imaging patterns. Some of these cases are possibly due to mutations in the protein biosynthetic pathway in the endoplasmic reticulum.[25] Other possible causes for these atypical cases are thought to be due to somatic mosaicism, which often leads to complete sparing of cystic kidney disease with normal parenchyma in multiple portions of the kidney.[25,26] Somatic mosaicism refers to the occurrence of two genetically distinct populations of cells within an individual, derived from a postzygotic mutation after embryogenesis.[27,28] These mutations from the mosaicism may involve the germ line and the somatic cells. Somatic mosaicism is suggested to be one of the mechanisms that leads to ADPKD cases with atypical imaging patterns, such as asymmetric, unilateral, and lopsided patterns.[29] Somatic mosaicism may also lead to cases with less apparent family history. Iliuta *et al.* previously concluded, from their study of 209 patients, that cases without an apparent family history may be due to *de novo* disease, germline or somatic mosaicism, or mild disease from hypomorphic PKD1 and PKD2 mutations.[30] Interestingly, 16.3% (34 of 209) of patients displayed an atypical imaging pattern.[30]

The genetics analysis of these atypical cases in our cohort would be the next phases for our study. The genotype among the atypical cases in our cohort would certainly be of interest, as gene variants, such as in *DNAJB11* and *ALG5*, have recently been discovered as a causes of atypical polycystic kidney disease.[19,31] The genetic complexity and heterogeneity in ADPKD has been highlighted in a recent review[32] and in two recent cohorts with exome sequencing performed.[33,34]

The strength of our study is that this is a detailed cohort analysis of a Chinese population with ADPKD with systematic baseline MRI and documented imaging patterns. Our cohort also consisted of a population with unrelated individuals and is essentially treatment-naïve. The limitations of our cohort include the relatively small size and short follow-up duration, complicating the assessment of kidney function decline among different morphologies. The small size in each of the subclasses and the insufficient follow-up in our cohort did not allow us to observe any statistically significant differences in the 40% decline in eGFR among each subclasses. Thus, a study with larger size and a longer follow-up would be required to assess 40% decline in eGFR among the different subclasses. Efforts have been done to assess the validity of various eGFR estimating equations to determine differences in the natural history of disease progression in ADPKD,[35] which we have not investigated in our study with a Chinese cohort. However, the evaluation of renal function with these formulas in patients with ADPKD is currently unreliable, and certainly none of these equations have been validated in Chinese.

A multicentre observational cohort (the CysticHK cohort) involving 13 tertiary hospitals in Hong Kong is underway. We do not have the genotype information on the cohort yet, but genetics analysis is underway and would hopefully give us a more information on the genotype–phenotype correlation among the typical and atypical patterns in this cohort. In summary, our study provides baseline characterization and detailed MRI patterns in a Chinese cohort with ADPKD. These results pave the way for a larger ADPKD registry in Hong Kong, with the prospect of more detailed genotype–phenotype correlations advancing risk stratification and management in ADPKD.

Disclosures

Disclosure forms, as provided by each author, are available with the online version of the article at http://links.lww.com/KN9/A475.

Funding

This work was supported by Chinese University of Hong Kong (6905134 and 7101215) and Drs. Richard Charles and Ester Yewpick Lee Charitable Foundation.

Acknowledgments

We would also like to express our heartfelt gratitude to the Hong Kong Society of Nephrology for their support and for their 35th Anniversary Research Grant.

The funders had no role in study design, data collection and analysis, decision to publish, or preparation of the manuscript.

Author Contributions

Conceptualization: Winston Wing-Shing Fung.
Data curation: Phyllis Mei-Shan Cheng, Winston Wing-Shing Fung.
Formal analysis: Winston Wing-Shing Fung.
Funding acquisition: Winston Wing-Shing Fung, Philip Kam-Tao Li.
Investigation: Winston Wing-Shing Fung.
Methodology: Winston Wing-Shing Fung.
Project administration: Philip Kam-Tao Li.
Resources: Phyllis Mei-Shan Cheng, Kai-Ming Chow, Winnie Chiu-Wing Chu, Vickie Wai-Ki Kwong, Sam Lik-Fung Lau, Wing-Fai Pang.
Supervision: Kai-Ming Chow, Olivier Devuyst, Philip Kam-Tao Li, Albert Chee Meng Ong, Cheuk-Chun Szeto.
Writing – original draft: Winston Wing-Shing Fung.
Writing – review & editing: Olivier Devuyst, Winston Wing-Shing Fung, Philip Kam-Tao Li, Albert Chee Meng Ong, Cheuk-Chun Szeto.

Data Sharing Statement

All data are included in the manuscript and/or supporting information.

Supplemental Material

This article contains the following supplemental material online at http://links.lww.com/KN9/A474.

Supplemental Table 1. Classification of patients with ADPKD by prespecified imaging according to Mayo classification.

References

1. Lanktree MB, Haghighi A, Guiard E, et al. Prevalence estimates of polycystic kidney and liver disease by population sequencing. *J Am Soc Nephrol.* 2018;29(10):2593–2600. doi:10.1681/ASN.2018050493
2. Chebib FT, Torres VE. Autosomal dominant polycystic kidney disease: core curriculum 2016. *Am J Kidney Dis.* 2016;67(5):792–810. doi:10.1053/j.ajkd.2015.07.037
3. Pei Y, Obaji J, Dupuis A, et al. Unified criteria for ultrasonographic diagnosis of ADPKD. *J Am Soc Nephrol.* 2009;20(1):205–212. doi:10.1681/ASN.2008050507
4. Lanktree MB, Guiard E, Li W, et al. Intrafamilial variability of ADPKD. *Kidney Int Rep.* 2019;4(7):995–1003. doi:10.1016/j.ekir.2019.04.018
5. Chebib FT, Perrone RD, Chapman AB, et al. A practical guide for treatment of rapidly progressive ADPKD with tolvaptan. *J Am Soc Nephrol.* 2018;29(10):2458–2470. doi:10.1681/ASN.2018060590
6. Irazabal MV, Rangel LJ, Bergstralh EJ, et al.; CRISP Investigators. Imaging classification of autosomal dominant polycystic kidney disease: a simple model for selecting patients for clinical trials. *J Am Soc Nephrol.* 2015;26(1):160–172. doi:10.1681/ASN.2013101138
7. Xue C, Zhou C, Mei C. Total kidney volume: the most valuable predictor of autosomal dominant polycystic kidney disease progression. *Kidney Int.* 2018;93(3):540–542. doi:10.1016/j.kint.2017.10.027
8. Yu ASL, Shen C, Landsittel DP, et al.; Consortium for Radiologic Imaging Studies of Polycystic Kidney Disease CRISP. Baseline total kidney volume and the rate of kidney growth are associated with chronic kidney disease progression in autosomal dominant polycystic kidney disease. *Kidney Int.* 2018;93(3):691–699. doi:10.1016/j.kint.2017.09.027
9. Grantham JJ, Torres VE, Chapman AB, et al.; CRISP Investigators. Volume progression in polycystic kidney disease. *N Engl J Med.* 2006;354(20):2122–2130. doi:10.1056/NEJMoa054341
10. Chen D, Ma Y, Wang X, et al. Clinical characteristics and disease predictors of a large Chinese cohort of patients with autosomal dominant polycystic kidney disease. *PLoS One.* 2014;9(3):e92232. doi:10.1371/journal.pone.0092232
11. Ong AC, Devuyst O, Knebelmann B, Walz G.; ERA-EDTA Working Group for Inherited Kidney Diseases. Autosomal dominant polycystic kidney disease: the changing face of clinical management. *Lancet.* 2015;385(9981):1993–2002. doi:10.1016/S0140-6736(15)60907-2
12. Petzold K, Gansevoort RT, Ong AC, et al. Building a network of ADPKD reference centres across Europe: the EuroCYST initiative. *Nephrol Dial Transplant.* 2014;29(suppl 4):iv26–32. doi:10.1093/ndt/gfu091
13. Oh YK, Ryu H, Ahn C, et al.; RAPID-ADPKD Study Group. Clinical characteristics of rapid progression in asia-Pacific patients with ADPKD. *Kidney Int Rep.* 2023;8(9):1801–1810. doi:10.1016/j.ekir.2023.06.018
14. Mei CL, Xue C, Yu SQ, et al. Executive summary: clinical practice guideline for autosomal dominant polycystic kidney disease in China. *Kidney Dis (Basel).* 2020;6(3):144–149. doi:10.1159/000506288
15. Yu CC, Lee AF, Kohl S, et al.; Taiwan PKD Consortium. PKD2 founder mutation is the most common mutation of polycystic kidney disease in Taiwan. *NPJ Genom Med.* 2022;7(1):40. doi:10.1038/s41525-022-00309-w
16. Bae KT, Shi T, Tao C, et al.; HALT PKD Consortium. Expanded imaging classification of autosomal dominant polycystic kidney disease. *J Am Soc Nephrol.* 2020;31(7):1640–1651. doi:10.1681/ASN.2019101121
17. Alam A, Dahl NK, Lipschutz JH, et al. Total kidney volume in autosomal dominant polycystic kidney disease: a biomarker of disease progression and therapeutic efficacy. *Am J Kidney Dis.* 2015;66(4):564–576. doi:10.1053/j.ajkd.2015.01.030
18. Torres VE, Harris PC, Pirson Y. Autosomal dominant polycystic kidney disease. *Lancet.* 2007;369(9569):1287–1301. doi:10.1016/S0140-6736(07)60601-1
19. Porath B, Gainullin VG, Cornec-Le Gall E, et al.; Genkyst Study Group HALT Progression of Polycystic Kidney Disease Group-Consortium for Radiologic Imaging Studies of Polycystic Kidney Disease. Mutations in GANAB, encoding the glucosidase IIα subunit, cause autosomal-dominant polycystic kidney and liver disease. *Am J Hum Genet.* 2016;98(6):1193–1207. doi:10.1016/j.ajhg.2016.05.004
20. van de Laarschot LFM, Te Morsche RHM, Hoischen A, et al. Novel GANAB variants associated with polycystic liver disease. *Orphanet J Rare Dis.* 2020;15(1):302. doi:10.1186/s13023-020-01585-4
21. Pisani I, Allinovi M, Palazzo V, et al. More dissimilarities than affinities between DNAJB11-PKD and ADPKD. *Clin Kidney J.* 2022;15(6):1179–1187. doi:10.1093/ckj/sfac032
22. Lemoine H, Raud L, Foulquier F, et al, Genomics England Research Consortium, Genkyst Study Group. Monoallelic pathogenic ALG5 variants cause atypical polycystic kidney disease and interstitial fibrosis. *Am J Hum Genet.* 2022;109(8):1484–1499. doi:10.1016/j.ajhg.2022.06.013
23. Besse W, Chang AR, Luo JZ, et al.; Regeneron Genetics Center. ALG9 mutation carriers develop kidney and liver cysts. *J Am Soc Nephrol.* 2019;30(11):2091–2102. doi:10.1681/ASN.2019030298

24. Senum SR, Li YSM, Benson KA, et al.; Genomics England Research Consortium the HALT PKD CRISP DIPAK ADPKD Modifier and TAME PKD studies. Monoallelic IFT140 pathogenic variants are an important cause of the autosomal dominant polycystic kidney-spectrum phenotype. *Am J Hum Genet.* 2022;109(1):136–156. doi:10.1016/j.ajhg.2021.11.016
25. Lanktree MB, Haghighi A, di Bari I, Song X, Pei Y. Insights into autosomal dominant polycystic kidney disease from genetic studies. *Clin J Am Soc Nephrol.* 2021;16(5):790–799. doi:10.2215/CJN.02320220
26. Hopp K, Cornec-Le Gall E, Senum SR, et al.; HALT Progression of Polycystic Kidney Disease Group the ADPKD Modifier Study. Detection and characterization of mosaicism in autosomal dominant polycystic kidney disease. *Kidney Int.* 2020;97(2):370–382. doi:10.1016/j.kint.2019.08.038
27. Freed D, Stevens EL, Pevsner J. Somatic mosaicism in the human genome. *Genes (Basel).* 2014;5(4):1064–1094. doi:10.3390/genes5041064
28. Campbell IM, Shaw CA, Stankiewicz P, Lupski JR. Somatic mosaicism: implications for disease and transmission genetics. *Trends Genet.* 2015;31(7):382–392. doi:10.1016/j.tig.2015.03.013
29. Devuyst O, Pei Y. Next-generation sequencing for detection of somatic mosaicism in autosomal dominant polycystic kidney disease. *Kidney Int.* 2020;97(2):261–263. doi:10.1016/j.kint.2019.11.019
30. Iliuta IA, Kalatharan V, Wang K, et al. Polycystic kidney disease without an apparent family history. *J Am Soc Nephrol.* 2017;28(9):2768–2776. doi:10.1681/ASN.2016090938
31. Cornec-Le Gall E, Olson RJ, Besse W, et al.; Genkyst Study GroupHALT Progression of Polycystic Kidney Disease GroupConsortium for Radiologic Imaging Studies of Polycystic Kidney Disease. Monoallelic mutations to DNAJB11 cause atypical autosomal-dominant polycystic kidney disease. *Am J Hum Genet.* 2018;102(5):832–844. doi:10.1016/j.ajhg.2018.03.013
32. Cornec-Le Gall E, Torres VE, Harris PC. Genetic complexity of autosomal dominant polycystic kidney and liver diseases. *J Am Soc Nephrol.* 2018;29(1):13–23. doi:10.1681/ASN.2017050483
33. Schönauer R, Baatz S, Nemitz-Kliemchen M, et al. Matching clinical and genetic diagnoses in autosomal dominant polycystic kidney disease reveals novel phenocopies and potential candidate genes. *Genet Med.* 2020;22(8):1374–1383. doi:10.1038/s41436-020-0816-3
34. Chang AR, Moore BS, Luo JZ, et al. Exome sequencing of a clinical population for autosomal dominant polycystic kidney disease. *JAMA.* 2022;328(24):2412–2421. doi:10.1001/jama.2022.22847
35. Rodríguez RM, Luis-Lima S, Fernandez JM, et al. Estimated GFR in autosomal dominant polycystic kidney disease: errors of an unpredictable method. *J Nephrol.* 2022;35(8):2109–2118. doi:10.1007/s40620-022-01286-0